A New Approach to the Stability Analysis of Boost Power-Factor-Correction Circuits

SUDIP K. MAZUMDER

Department of Electrical and Computer Engineering, University of Illinois, MC 154, 851 South Morgan Street, Chicago, IL 60607-7053, USA

ALI H. NAYFEH

Department of Engineering Science and Mechanics, MC 0219, Virginia Polytechnic Institute and State University, Blacksburg, VA 24061, USA

Abstract : We analyze the stability of a boost power-factor-correction (PFC) circuit using a hybrid model. We consider two multi-loop controllers to control the power stage. For each closed-loop system, we treat two separate cases: one for which the switching frequency is approaching infinity and the other for which it is finite but large. Unlike all previous analyses, the analysis in this paper investigates the stability of the converter in the saturated and unsaturated regions of operation. Using concepts of discontinuous systems, we show that the global existence of a smooth hypersurface for the boost PFC circuit is not possible. Subsequently, we develop conditions for the local existence of each of the closed-loop systems using a Lyapunov function. In other words, we derive the conditions for which a trajectory will reach a smooth hypersurface. If the trajectories do not reach the sliding surface, then the system saturates. As such, the stability of the period-one orbit is lost. Using the conditions for existence and the concept of equivalent control, we show why, for the second closed-loop system, the onset of the fast-scale instability occurs when the inductor current approaches zero. For this system, we show that the onset of the fast-scale instability near zero-inductor current occurs for a lower line voltage. Besides, when the peak of the line voltage approaches the bus voltage, the fast-scale instability may occur not only at the peak but also when the inductor current approaches zero. We develop a condition which ensures that the saturated region does not have any stable orbits. As such, a solution that leaves the sliding surface (if existence fails) cannot stabilize in the saturated region. Finally, we extend the analysis to the case in which the converter operates with a finite but large switching frequency. As such, the system has two fundamental frequencies: the switching and line frequencies. Hence, the dynamics of the system evolve on a torus. We show two different approaches to obtaining a solution for the closed-loop system. For the second closed-loop system, using the controller gain for the current loop as a bifurcation parameter, we show (using a Poincaré map) the mechanism of the torus breakdown. If the mechanism of the torus breakdown is known, then, depending on the post-instability dynamics, a designer can optimize the design of the closed-loop converter.

Key Words : Bifurcation analysis, PFC circuits, discontinuous systems, sliding-mode control, Lyapunov method

1. INTRODUCTION

Power-factor-correction (PFC) circuits are widely used in power electronics. One of the most common circuits used to achieve unity power factor is the time-varying boost PFC circuit, which is shown in Figure 1. The operation of the converter has been analyzed in detail by many researchers (Mohan et al., 1984; Henze and Mohan, 1986; Ridley, 1989; Williams, 1989; Zhou et al., 1990; Zhou and Jovanović, 1992; Huliehel et al., 1992; Simonetti et al., 1995). However, very few have even attempted to properly analyze the stability of this system. As discussed in Section 2, the system of equations for the boost PFC circuit involves discontinuity in control and non-differentiability in state and time. These qualities, in addition to the time-varying nature of the converter, make the analysis of the boost PFC circuit difficult.

Some researchers have analyzed the stability of this time-varying system using a smooth linearized small-signal model. Mohan et al. (1984) used the concept of quasi-static analysis to analyze the current-loop stability of the boost PFC circuit operating with hysteretic control. Ridley (1989) and Williams (1989) developed a small-signal model to facilitate the design of an output-voltage compensator for resistive and constant-power loads. A more concrete small-signal analysis is given by Huliehel et al. (1992); they justify their analysis by replacing the time-varying input voltage with a nonlinear feedforward control. They developed a small-signal model for the boost PFC circuit, operating with a constant switching frequency, for the design and analysis of the voltage and current loops. Zhou and Jovanović (1992) demonstrated the current-loop instabilities occurring in the boost PFC circuit operating with peak-current-mode control and with average-current-mode control.

There are some major shortcomings in these analyses. First, they assume that, when the power is fed to the converter, the trajectories of the system will approach a sliding surface (see Section 3 for definition) and remain on it. In other words, the sliding surface is assumed to always exist (Filippov, 1988; Utkin, 1992). This may not be true, even for systems that are linear with respect to control and systems which may have a real equilibrium solution or a stable orbit in the saturated region. Secondly, the averaged model completely neglects the impact of the switching frequency and hence cannot predict the dynamics on the fast scale (Mazumder et al., 2001). We have demonstrated in our earlier papers that instability in either a standalone or an integrated converter can occur on a fast scale as well as on a slow scale (Alfayyoumi et al., 1999; Mazumder et al., 2001). Thirdly, even the slow-scale averaged model may have more than one equilibrium solution or more than one stable orbit. However, a linearized small-signal analysis ignores the presence of these other solutions. Therefore, a small-signal analysis cannot predict anything about the domain of attraction of the nominal solution or orbit. For example, the averaged model of a multi-loop dc–dc boost converter may have a quadratic nonlinearity (Erickson et al., 1982). Hence, this system may have more than one equilibrium solution. If two of these solutions are stable, then the system will have two operating points, one of which is the nominal solution. This possibility is completely ignored in linearized averaged models. Consequently, the small-signal model cannot predict the post-instability dynamics. Besides, controllers that are designed based on this model may be conservative and may not yield globally stable closed-loop systems.

In this paper, we begin by developing a state-space model for the boost PFC circuit, which is designed to operate in the continuous-conduction mode (CCM). Although the converter operates in CCM, when the input voltage is low, the inductor current becomes zero during a
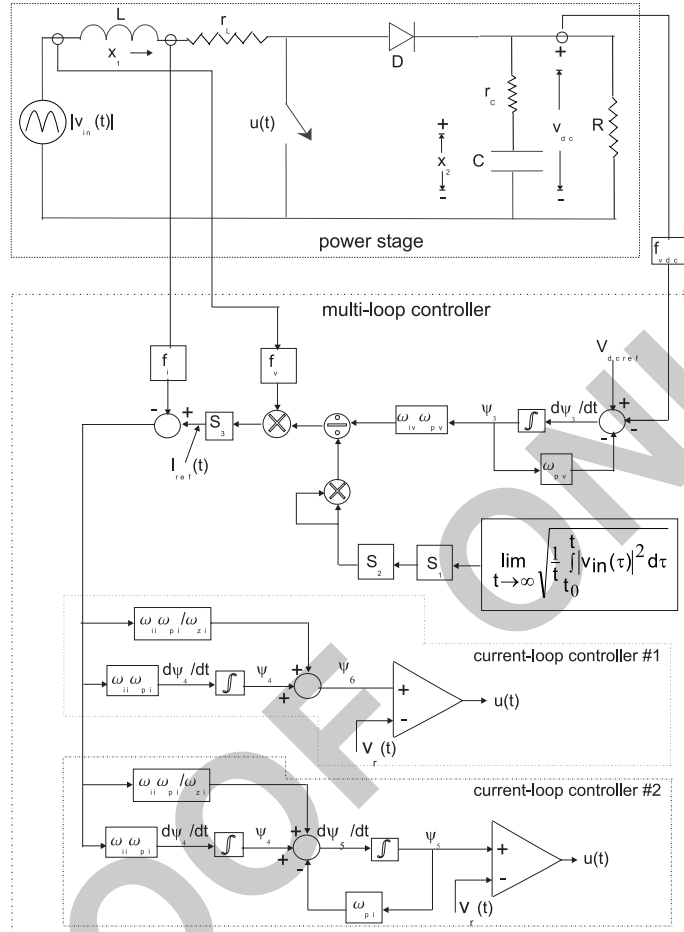
Figure 1. A closed-loop boost PFC circuit. We consider two different multi-loop controllers to control the power stage.

small interval, and the converter operates in the discontinuous-conduction mode (DCM) in that interval. With a proper choice of the circuit parameters, this duration can be minimized, but for a feasible converter it cannot be made zero. Consequently, we show that global existence of a smooth hypersurface is not possible. In other words, the trajectories of the system do not reach the sliding surface for all of the initial conditions. As such, the system saturates and the stability of the period-one orbit is lost. Using the developed model of the boost PFC, we analyze the stability and dynamics of the converter in the saturated and unsaturated regions using the Lyapunov method and a bifurcation analysis. Our analysis predicts not only the instabilities, but also their mechanism. Our general stability analysis does not require the forcing function (or the input voltage) to be harmonic (e.g., $\cos \omega t$), which has been a common feature in previous analyses. However, we show that, if we make such an assumption, then we can compute the exact solution of the time-varying system.

2. MODEL OF THE CLOSED-LOOP CONVERTER

The boost PFC circuit designed to operate in CCM, see Figure 1, switches between three structures. The jump between two of these structures is governed by the switching function $u(t)$. The system attains the third structure only when the inductor current $x_1(t)$ is zero and hence $u(t)$ has no control over it. In general, the inductor current and the input voltage $(v_{in}(t))$ approach zero simultaneously. We should note that the inductor current in a boost PFC circuit designed solely for the DCM attains a value of zero in every switching cycle (of period $T = \frac{1}{f_s}$).

We describe the dynamics of the open-loop states of the boost PFC circuit (operating in CCM) using the following hybrid equations

$$
\begin{aligned}
\dot{x}_1(t) &= \left[-\frac{1}{L}\left(r_L + \frac{r_C R}{R + r_C}\left(1 - u(t)\right)\right) x_1(t) \right. \\
&\qquad \left. -\frac{1}{L}\frac{R}{R + r_C}\left(1 - u(t)\right)x_2(t) + \frac{1}{L}|v_{in}(t)| \right] g_1\left(x_1(t), u(t)\right) \\
\dot{x}_2(t) &= \frac{R}{(R + r_C)C}\left(1 - u(t)\right)x_1(t) - \frac{1}{(R + r_C)C}x_2(t)
\end{aligned}
\tag{1}
$$

where $x_2(t)$ is the voltage across the capacitor, r_c and r_c are parasitic resistances of the inductor and the output capacitor, and

$$
g_1\left(x_1(t), u(t)\right) = \begin{cases} 1 & \text{if } x_1(t) > 0 \\ 1 & \text{if } x_1(t) = 0, u(t) = 1 \\ 0 & \text{if } x_1(t) = 0, u(t) = 0 \end{cases}.
\tag{2}
$$

For an open-loop converter, $u(t)$ is a pre-determined pulse function. For a closed-loop converter, $u(t)$ is a function of the states of the power stage for a static feedback controller and is a function of the states of the controller and the power stage for a dynamic feedback controller. The objectives of the closed-loop converter are to regulate the bus voltage and to draw line current from the utility in synchronicity with the input voltage. There are numerous ways to design the feedback controller. Although our analysis can be extended to any other controller, we select two multi-loop controllers, one of which (controller II) is already being used in a commercial product (Andreycak, 1997; Todd, 1999). The voltage-loop controller for both multi-loop controllers is the same. However, the current-loop controllers are slightly different.

As shown in Figure 1, the closed-loop system has an outer voltage loop and an inner current loop. The voltage loop provides the reference for the inner current loop. The mathematical model describing feedback controller I is given by

$$
\begin{aligned}
\dot{\psi}_3(t) &= -f_{vdc}\, v_{dc}(t) - \omega_{pv}\, \psi_3(t) + V_{dcref} \\
\dot{\psi}_4(t) &= \lambda_1(t)\psi_3(t) - \lambda_2 x_1(t)
\end{aligned}
\tag{3}
$$

where

$$\dot{\psi}_5(t) = -\lambda_3 x_1(t) + \lambda_4(t)\psi_3(t) + \psi_4(t) - \omega_{pi}\psi_5(t)$$

$$v_{dc}(t) = \frac{R}{R+r_C}x_2(t) + \frac{Rr_C}{R+r_C}\Big(1 - u(t)\Big)x_1(t).$$

In equation (3), $\psi_i(t)$ represent the states of the dynamic feedback controller, f_{vdc} is the sensor gain for the bus voltage, and V_{dcref} is the reference for the bus voltage. The coefficients $\lambda_i(t)$ are positive, bounded, and given by

$$\lambda_1(t) = \omega_{ii}\omega_{pi}\frac{\omega_{iv}\omega_{pv}}{S_1^2 S_2^2 \left(\frac{1}{t}\int_{t_0}^{t}|v_{in}(\tau)|^2 d\tau\right)}f_v|v_{in}(t)|S_3,$$

$$\lambda_2 = \omega_{ii}\omega_{pi}f_i, \quad \lambda_3 = \frac{\lambda_2}{\omega_{zi}}, \quad \text{and} \quad \lambda_4(t) = \frac{\lambda_1(t)}{\omega_{zi}} \qquad (4)$$

where f_v and f_i are the sensor gains for the line voltage and inductor currents, respectively, and $S_1, S_2,$ and S_3 are feedback gains for the voltage and current loops. For convenience, we represent $x(t)$, $\psi(t)$, and $u(t)$ as x, ψ, and u from now on.

The switching function is defined as

$$u(t) = \begin{cases} 1 & \text{if } \sigma_1 > v_r(t) \\ 0 & \text{if } \sigma_1 < v_r(t) \end{cases} \qquad (5)$$

where $\sigma_1 = \phi_6$ for controller I, $\sigma_1 = \psi_5$ for controller II, $v_r(t) = v_l + v_{ramp} \bmod(t, T)f_s$, and v_l and v_{ramp} are the lower limit and height of the ramp. The function ϕ_6 is defined in Figure 1. In equation (5), $v_r(t)$ represents the carrier waveform (ramp) and creates a time-varying boundary layer.

3. CONCEPTS OF DISCONTINUOUS SYSTEMS

The condition for the existence of the ith discontinuity surface ($\sigma_i = 0$) of a differential equation

$$\dot{y} = f(y, t, u) \qquad (6)$$

with discontinuous right-hand side in the neighborhood of $\sigma_i = 0$ is (Utkin, 1992)

$$\lim_{\sigma_i \to -0} \dot{\sigma}_i > 0 \quad \text{and} \quad \lim_{\sigma_i \to +0} \dot{\sigma}_i < 0 \qquad \text{or} \qquad \dot{\sigma}_i\sigma_i < 0. \qquad (7)$$

If the hypersurface exists globally, then all of the solutions of equation (6) in the continuity region reach it and remain on it. The motion on the discontinuity surface is known as a sliding mode, and hence the discontinuity surface is also known as a sliding surface (or smooth hypersurface) (Utkin, 1992; Filippov, 1988). If the sliding surface does not exist globally, then the solutions may not reach it.

In Figure 2, using a single discontinuity surface given by $\sigma_1 = 0$, we show some possible trajectories when global existence fails. The trajectories marked T_1 reach the discontinuity surface from both sides. Hence they satisfy equation (6). The trajectories marked T_2 do
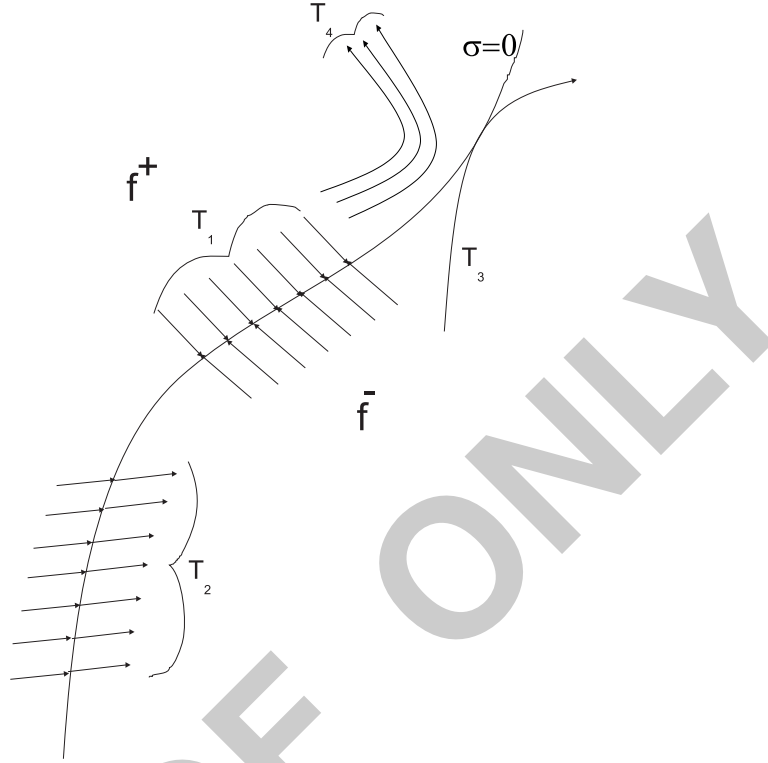
Figure 2. Some possible trajectories for the variable-structure system described by equation (6). Only T_1 satisfies the existence condition, T_4 remains in the saturated/continuity region.

not reach the discontinuity surface from both sides. Although these trajectories reach the discontinuity surface, they do not satisfy the existence condition. The trajectories marked T_3 approach the sliding surface tangentially and hence do not satisfy equation (6) because the velocity vectors on both sides of the discontinuity surface have the same sign. Finally, T_4 represents the set of trajectories which do not reach the discontinuity surface at all.

When the global existence of a sliding surface fails, it is still possible that the discontinuity surface may satisfy equation (6) locally. If, in addition, the saturated region does not have real equilibrium solution(s) or stable orbit(s), then a solution that leaves the local sliding surface cannot stabilize in the saturated region. For example, a piecewise linear boost dc–dc converter feeding a resistive load may have one equilibrium solution in the saturated region (Mazumder et al., 2001, 2002). Hence, the dynamics of an improperly designed boost converter may be attracted by this solution if subjected to a strong disturbance. If the resistive load is replaced with a constant-power load, then the saturated region may have more than one equilibrium solution.

Once we have demonstrated that a sliding surface exists locally or globally, we analyze the stability of the system dynamics on the sliding surface. For the continuity region, the definition of a solution is clear (Filippov, 1988). However, the definition of a solution (almost everywhere) as an absolutely continuous function satisfying (6) is not always applicable for

equations whose right-hand sides are discontinuous on an arbitrary smooth surface. Using the Lebesgue measure, we can apply the definition in the case in which the solutions approach the discontinuity surface on one side and leave it on the other side. When the solutions approach a discontinuity surface on both sides, the conventional definition is unsuitable because there is no indication of how a solution that reaches the discontinuity surface may continue.

Filippov (1988) defined a solution for the vector differential equation

$$\dot{y} = f(y, t, u(y)) = h(y, t) \tag{8}$$

where $h : \Re^n \times \Re \to \Re^n$ is measurable and essentially locally bounded. A vector function $y(t)$, defined on the interval (t_1, t_2), is a Filippov solution of equation (8) if it is absolutely continuous and, for almost all $t \in (t_1, t_2)$ and for arbitrary $\delta > 0$, the vector $dy(t)/dt$ belongs to the smallest convex closed set of an n-dimensional space containing all of the values of the vector function $h(y', t)$; where y' ranges over the entire δ neighborhood of the point $y(t)$ in the space y (with t fixed) except for a set N of measure $\mu N = 0$; that is,

$$\frac{dy(t)}{dt} \in K[h](y, t) \tag{9}$$

where $K[h](.)$ is called the Filippov differential inclusion and is defined as

$$K[h](y, t) \equiv \bigcap_{\delta > 0} \bigcap_{\mu N = 0} \overline{co}\, h\left(B(y, \delta) - N\right). \tag{10}$$

In differential inclusion (10), $\overline{co}$ denotes the convex hull of a set, N represents a set of zero Lebesgue measure, μN and B is a ball of radius δ centered at y. The content of the Filippov solution is that the tangent vector to a solution at a time t, where it exists, must lie in the convex closure of the limiting values of the vector field in progressively smaller neighborhoods around the solution evaluated at time t.

Let us consider a single switching surface H (shown in Figure 3), which is a smooth surface (manifold) separating the space into regions H^+ and H^-. Suppose that H is regular so that it can be defined by a smooth real-valued function $\sigma(y)$ (i.e., $H = \{y : \sigma(y) = 0\}$ and suppose that $h(y, t)$ is bounded and, for any fixed t, its limiting values $h^+(y, t)$ and $h^-(y, t)$ exist when H is approached from H^+ and H^-. Let $h_0^+(y, t)$ and $h_0^-(y, t)$ be the projections of $h^+(y, t)$ and $h^-(y, t)$ on the normal $\bigtriangledown \sigma$ to the surface H directed towards H^+ and H^-. Then, for an absolutely continuous $y \in H$ satisfying $h_0^+(y, t) \leq 0$, $h_0^-(y, t) \geq 0$, and $h_0^-(y, t) - h_0^+(y, t) > 0$, the trajectories pointing towards H are solutions of equation (8) according to the differential inclusion (9) if and only if

$$\frac{dy}{dt} = \beta(t)h^+(y, t) + (1 - \beta(t))h^-(y, t) \tag{11}$$

where

$$\beta(t) = \frac{h_0^-(y, t)}{h_0^-(y, t) - h_0^+(y, t)}. \tag{12}$$

We note that the right-hand side of equation (11) is orthogonal to $\bigtriangledown \sigma$ and hence the solution remains on the surface H.
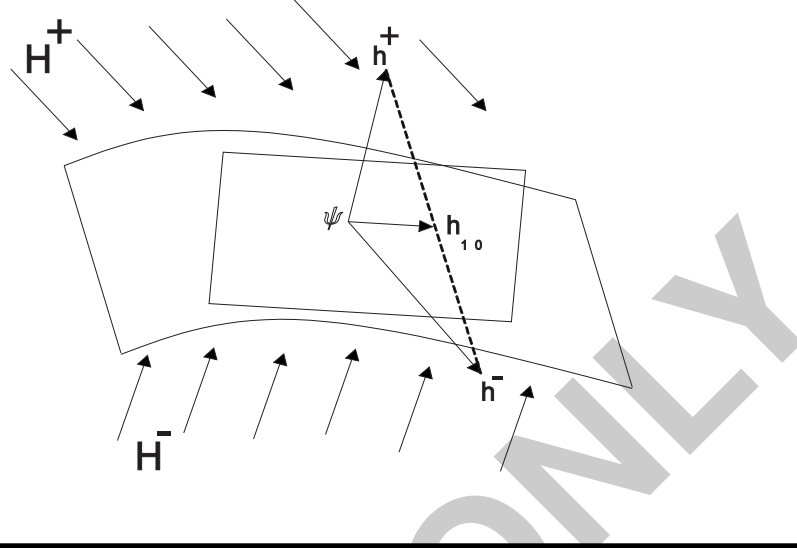
Figure 3. A description of the Filippov solution (often called sliding motion) on the discontinuity surface σ.

The sliding mode in a real-life system actually occurs not on its discontinuity surface, but within some boundary layer on which the control components may take values different from u_i^+ and u_i^- (Utkin, 1992). The vector $f(y,t,u)$ in equation (6) may, therefore, take values which differ from those obtained with $u_i = u_i^+$ and $u_i = u_i^-$. This results in a wider convex set in the Filippov continuation method and, consequently, in a richer set of motions on the sliding mode. In order to handle the regularization problem and find feasible solutions to equation (6), Utkin (1992) proposed an equivalent control method.

We assume that a sliding mode exits on the manifold

$$\sigma(y) = 0, \qquad \sigma^{T}(y) = [\sigma_1(y), \cdots, \sigma_m(y)] \tag{13}$$

which lies at intersection of m discontinuity surfaces. Then, we can find a continuous control such that, under the initial position of the state vector on this manifold, the time derivative of the vector $\sigma(y)$ along the trajectories of system equation (6) is identically zero; that is,

$$\dot{\sigma} = \bigtriangledown \sigma_y f(y,t,u_1^{eq}(y,t), \cdots, u_m^{eq}(y,t)) = 0. \tag{14}$$

In equation (14), $u^{eq}(y) = [u_1^{eq}, \cdots, u_m^{eq}]$ is referred to as the equivalent control for the vector equation (6) on the sliding surface $\sigma(y) = 0$. Therefore, the dynamics of equation (6) on the sliding surface are governed by

$$\dot{y} = f[y,t,u^{eq}(y,t)]. \tag{15}$$

Thus, a solution is an absolutely continuous vector-valued function, which outside the surfaces σ_i satisfies equation (6) and on these surfaces and on their intersections satisfies equation (15) for almost all t.

For a system which is linear with respect to control, when the width of the boundary layer is zero, the solutions obtained using the equivalent control method and the Filippov method

are the same. The stability of the solutions of either equations (11) or (15) is determined using linear techniques if the sliding manifold is linear. If, however, the sliding manifold is nonlinear, then Lyapunov's first and second methods and bifurcation analysis are suitable approaches (Hahn, 1963; Nayfeh and Balachandran, 1995; Khalil, 1996).

4. ANALYSIS OF THE DISCONTINUOUS CONVERTER WHEN THE SWITCHING FREQUENCY APPROACHES INFINITY

We use the concepts of discontinuous systems to analyze the boost PFC circuit, the dynamics of which are described by equations (1)–(5). First, let us consider the closed-loop system operating with controller I. In this case, $\sigma_1 = \psi_6$ because $v_r(t) = 0$ for an infinite frequency. A sliding mode exists if the trajectories converge on $\psi_6 = 0$ (Utkin, 1992). Let us define a Lyapunov function

$$V(\psi_6) = \frac{1}{2}\psi_6{}^2 \tag{16}$$

so that the existence condition for the sliding surface is

$$\dot{V}(\psi_6) = \psi_6\dot{\psi}_6 \leq 0 \tag{17}$$

where

$$\dot{\sigma}_1 = \dot{\psi}_6 = \dot{\psi}_4 - \lambda_3\dot{x}_1 + \dot{\lambda}_4(t)\psi_3 + \lambda_4(t)\dot{\psi}_3 \tag{18}$$

$$\dot{\lambda}_4(t) = c_1 f_v S_3\left[\dot{v}_{in}(t)\mathrm{sign}(v_{in}(t))\frac{1}{\frac{1}{t}\int_{t_0}^t |v_{in}(\tau)|^2\mathrm{d}\tau} - |v_{in}(t)|\right.$$

$$\left.\left(\frac{1}{t}\int_{t_0}^t |v_{in}(\tau)|^2\mathrm{d}\tau\right)^{-2}\left(-\frac{1}{t^2}\int_{t_0}^t |v_{in}(\tau)|^2\mathrm{d}\tau + \frac{|v_{in}(t)|^2}{t}\right)\right] \tag{19}$$

and $c_1 = \left(\dfrac{\omega_{ii}\,\omega_{pi}\,\omega_{iv}\,\omega_{pv}}{\omega_{zi}\,S_1^2 S_2^2}\right)$. The derivative of $\lambda_4(t)$ is bounded even though $\dot{\lambda}_4(t)$ is not defined at $v_{in}(t) = 0$. Substituting for $\dot{x}_1, \dot{\psi}_3$, and $\dot{\psi}_4$ from equations (1) and (3) into equation (18) yields

$$\dot{\sigma}_1 = \dot{\psi}_6 = \lambda_4(t)V_{dcref} - \frac{\lambda_3 g_1}{L}|v_{in}| + \left(\lambda_1 + \lambda_4(t) - \dot{\lambda}_4(t)\omega_{pv}\right)\psi_3$$

$$- \left(\lambda_2 - \frac{\lambda_3 r_L g_1}{L}\right)x_1 - \frac{\lambda_4(t)f_{vdc}R}{R + r_c}x_2 + \frac{R}{L(R + r_c)}$$

$$\left[\lambda_3(r_c x_1 + x_2)g_1 - f_{vdc}Lr_c\lambda_4(t)x_1\right](1 - u). \tag{20}$$

We consider the possibility that the sliding surface exists globally. Then

$$u = u_{eq} + u_n \tag{21}$$

where u_{eq} is the equivalent control and u_n is the nonlinear switching control, which satisfies

$$u^- - u_{eq} \leq u_n \leq u^+ - u_{eq}. \tag{22}$$

The equivalent control u_{eq} is obtained by setting $\dot{\psi}_6 = 0$ in equation (20). The result is

$$u_{eq} = \frac{g_2}{f_{vdc}\, r_C\, L x_1 \lambda_4(t) - \lambda_3 g_1(x_1, u)\,(r_C x_1 + x_2)} \tag{23}$$

where

$$\begin{aligned}
g_2 &= \frac{L(R + r_c)}{R}\left[\lambda_4(t)V_{dcref} - \frac{\lambda_3 g_1}{L}\mid v_{in}\mid\right. \\
&\quad \left. + (\lambda_1 + \lambda_4(t) - \lambda_4(t)\omega_{pv})\,\psi_3 - \left(\lambda_2 - \frac{\lambda_3 r_L g_1}{L}\right)x_1 - \frac{f_{vdc} R\lambda_2}{R + r_c}x_2\right].
\end{aligned} \tag{24}$$

The functional g_2 is always defined and bounded for all x, ψ, and t. We know that for the sliding mode to exist

$$u^- < u_{eq} < u^+ \qquad (u^- = 0, \quad u^+ = 1). \tag{25}$$

It follows from equation (23) that, when $x_1 = 0$ and hence $g_1(x_1, u) = 0$, u_{eq} does not satisfy equation (25). Therefore, our assumption, that the sliding mode for the boost PFC circuit exists globally, is incorrect.

Having shown that global existence is not possible, we focus on the local existence of the sliding surface when $g_1(x_1, u) = 1$ (or $x_1 > 0$). We substitute equation (21) into equation (20), use equation (23), and obtain

$$\dot{\psi}_6 = ku_n \tag{26}$$

where

$$k = \frac{R}{L(R + r_c)}\left[(f_{vdc}\, L\lambda_4 - \lambda_3)\, r_c x_1 - \lambda_3 x_2\right]. \tag{27}$$

In equation (27), the term $f_{vdc}\, L\lambda_4(t)$ is negligible compared to $-\lambda_3(r_C x_1 + x_2)$ and hence $k < 0$ for all practical purposes. Then, it follows from equation (17) that for local existence

$$\dot{V}(\psi_6) = \psi_6\dot{\psi}_6 = \psi_6\,(ku_n) \leq 0. \tag{28}$$

Inequality (28) is satisfied if

$$\begin{aligned}
u_n &> 0\,(u^+ > u_{eq}) \quad \text{when} \quad \psi_6 > 0 \quad \text{and} \\
u_n &< 0\,(u^- < u_{eq}) \quad \text{when} \quad \psi_6 < 0.
\end{aligned} \tag{29}$$

Next we consider the boost PFC circuit operating with controller II. First, we consider the existence of the sliding surface. It follows from equation (5) and Figure 1 that when the width of the boundary layer is zero, u changes state when ψ_5 is less than or greater than

zero. Apparently $\psi_5 = 0$ is a sliding surface. Because $\dot{\psi}_5$ is a continuous function of time, the existence condition given by equation (7) is not satisfied. Thus, the sliding mode in the conventional sense (i.e., the trajectories being oriented towards the switching surface) does not exist. The existence condition may be derived from

$$\dot{\sigma}_1 = \dddot{\psi}_5 = -\lambda_3 \dot{x}_1 + \dot{\lambda}_4(t)\psi_3 + \lambda_4(t)\dot{\psi}_3 + \dot{\psi}_4 - \omega_{pi}\psi_5 \tag{30}$$

where $\dot{\lambda}_4(t)$ is given by equation (19). Substituting for $\dot{x}_1, \dot{\psi}_3,$ and $\dot{\psi}_5$ from equations (1) and (3) into equation (30), we have

$$\dot{\sigma}_1 = \dddot{\psi}_5 = \lambda_4 V_{dcref} - \frac{\lambda_3 g_1}{L} |v_{in}| + \left(\frac{\lambda_3 r_L g_1}{L} - \lambda_2 + \lambda_3 \omega_{pi} \right) x_1$$

$$- \frac{f_{vdc}\lambda_4 R}{R + r_c} x_2 + \left(\lambda_1 + \dot{\lambda}_4 - \lambda_4 \omega_{pi} \right) \psi_3 - \omega_{pi}\psi_4$$

$$+ \omega_{pi}^2 \psi_5 + \frac{R}{L(R + r_c)} \left[\lambda_3 g_1 x_2 + \lambda_3 r_c g_1 x_1 - f_{vdc}\lambda_4 r_c L x_1 \right] (1 - u). \tag{31}$$

A sliding mode exists if the trajectories converge on the origin in the plane $(\psi_5, \dot{\psi}_5)$ (Chang, 1990; Elmali and Olgac, 1992). We see from Figure 4(a) that for this higher-order sliding mode, all possible velocities lie in the space tangent to the manifold and, even when a switching error is present, the state trajectory is tangent to the manifold at the time of leaving, in contrast to the behavior of the closed-loop system operating with controller I. In the latter case, when a switching error is present, the trajectory leaves the manifold ($\dot{\psi}_6 = 0$) at a certain angle.

We consider the possibility that the sliding mode exists globally on the plane $(\psi_5, \dot{\psi}_5)$ for $g_1(x_1, u) = 0$. The equivalent control u_{eq} is obtained by solving $\dddot{\psi}_5 = 0$. The result is

$$u_{eq} = \frac{g_2}{\lambda_3(x_2 + r_c x_1)g_1 + f_{vdc}\lambda_4 r_c L x_1} \tag{32}$$

where

$$g_2 = \frac{L(R + r_c)}{R} \left[\lambda_4 V_{dcref} - \frac{\lambda_3 g_1}{L} |v_{in}| \right.$$

$$+ \left(\frac{\lambda_3 r_L g_1}{L} + \lambda_3 \omega_{pi} - \lambda_2 \right) x_1 - \frac{f_{vdc}\lambda_4 R}{R + r_c} x_2$$

$$\left. + \left(\lambda_1 + \dot{\lambda}_4 - \lambda_4 \omega_{pi} \right) \psi_3 - \omega_{pi}\psi_4 + \omega_{pi}^2 \psi_5 \right]. \tag{33}$$

For the nominal values of the states and the parameters in Tables 1 and 2, we find from equations (32) and (33) that

$$u_{eq} \approx 1 - \frac{|v_{in}|}{x_2} - \frac{\omega_{pi}}{g_1(x_2/L)\lambda_3} \left(\lambda_4 \psi_3 - \lambda_3 x_1 \right). \tag{34}$$
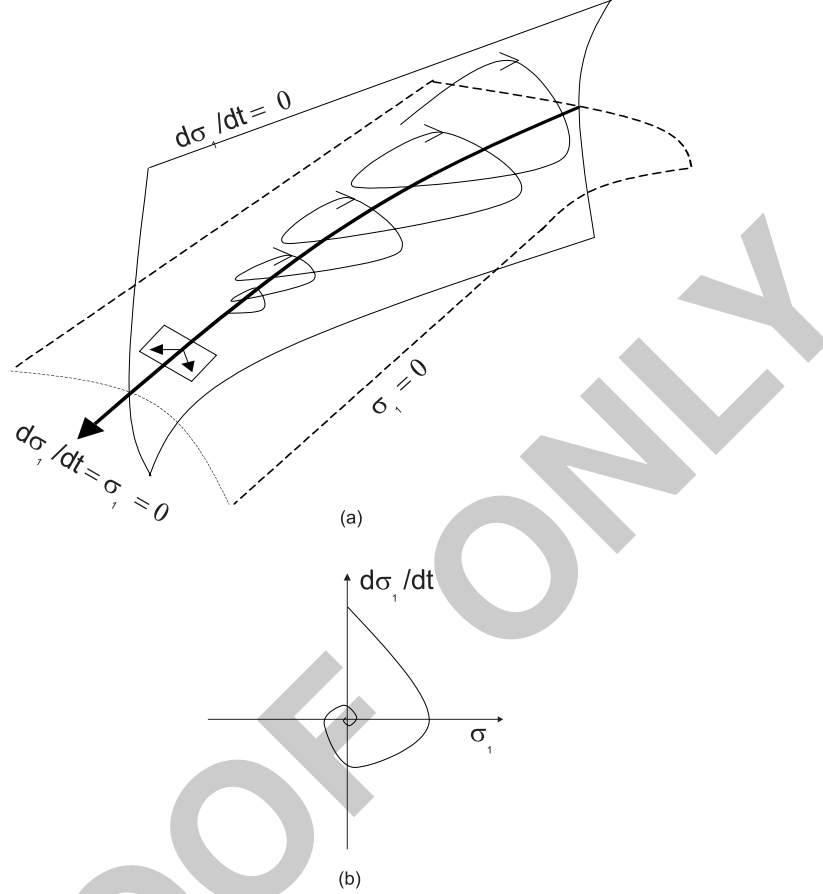
Figure 4. (a) A sliding-mode trajectory for the boost PFC circuit operating with current-loop controller number two. (b) A projection of the second-order sliding-mode trajectory on the plane $(\sigma_1, \dot{\sigma}_1)$.

It is obvious that u_{eq} obtained from equation (34) does not satisfy equation (25) when $x_1 = 0$. Therefore, global existence is not possible. We focus on the local existence of the sliding surface when $g_1(x_1, u) = 1$ (or $x_1 > 0$) and on the dynamics of the solutions once they leave the sliding surface. We choose the following positive definite Lyapunov function to find whether the solutions converge on the origin in the plane $(\psi_5, \dot{\psi}_5)$:

$$V(\psi_5, \dot{\psi}_5) = \frac{1}{2}\left(\psi_5^2 + \dot{\psi}_5^2\right). \tag{35}$$

Substituting equation (21) into equation (31) and using equations (32) and (33), we find that $\ddot{\psi}_5 = ku_n$, where k is defined in equation (27). Then, the local existence condition for the boost PFC circuit operating with controller II can be expressed as

$$\dot{V}(\psi_5, \dot{\psi}_5) = \dot{\psi}_5 \left(\psi_5 + \ddot{\psi}_5\right) = \dot{\psi}_5 \left(\psi_5 + ku_n\right) \leq 0. \tag{36}$$

Table 1. Power-stage parameters for the boost PFC circuit.

Parameter	Nominal Value
r_L	0.5 Ω
r_C	0.5 Ω
R	1000 Ω
L	1 mH
C	440 μF
f_s	90 kHz
ω	60 Hz
V_m	5.8 V
V_l	0.8 V

Table 2. Controller parameters for the boost PFC circuit.

Parameter	Nominal Value
V_{dcref}	3 V
f_i	0.25 A^{-1}
f_{Vdc}	$7.83807917 \times 10^{-3}$ V^{-1}
f_V	$6.67081869 \times 10^{-7}$ μA V^{-1}
S_1	0.9
S_2	0.326797385
S_3	3900 μA^{-1}
ω_{iv}	30.61974
ω_{pv}	14.1 Hz
ω_{ii}	3.5993418×10^5
ω_{zi}	9.7521411×10^3 Hz
ω_{pi}	1.0727355×10^5 Hz

We now analyze the existence condition (36) by considering the following two cases:

Case 1: $\left[\psi_5 > 0 \, (\psi_5 < 0) \Rightarrow u_n > 0 (u_n < 0), |k u_n| > |\psi_5| \right].$

For the boost PFC circuit, this is the operating condition for most of the time since k has a very large negative value. Hence,

$$\dot{V}(\psi_5, \dot{\psi}_5) = \dot{\psi}_5 \left(\psi_5 + k u_n \right) (\approx k u_n \dot{\psi}_5) \leq 0 \qquad \text{if} \qquad \dot{\psi}_5 \geq 0 \, (\dot{\psi}_5 \leq 0). \qquad (37a)$$

Case 2: $\left[\psi_5 > 0, -k u_n < \psi_5 \text{ or } \psi_5 < 0, -k u_n > \psi_5 \right].$

The condition for local existence in this case is

$$\dot{V}(\psi_5, \dot{\psi}_5) = \dot{\psi}_5 \left(\psi_5 + k u_n \right) (\approx \psi_5 \dot{\psi}_5) \leq 0 \qquad \text{if} \qquad \dot{\psi}_5 \leq 0 \, (\dot{\psi}_5 \geq 0). \qquad (37b)$$

Initially, if the closed-loop system satisfies $\ddot{\psi}_5 = \dot{\psi}_5 = \psi_5 = 0$ and if the switching frequency is infinite, then the closed-loop system is invariant in nature. However, if the frequency is anything but infinity and if the system is subjected to a perturbation, then because ψ_5 and $\dot{\psi}_5$ are continuous and $\psi_5 = \int \int \ddot{\psi}_5 \mathrm{d}\tau \mathrm{d}\beta$, $\dot{\psi}_5 = \int \ddot{\psi}_5 \mathrm{d}\tau$, the solutions do not converge immediately to $\ddot{\psi}_5 = \dot{\psi}_5 = \psi_5 = 0$. In fact, it is not possible to satisfy either equation (37a) or equation (37b) all the time if not at all. It is obvious from equations (34) and (37b) that the system is most vulnerable to instability when the conditions in Case 2 are achieved.

When the existence condition fails, then the solutions leave the sliding surface. If there exists a stable orbit in the saturated region, then there is a possibility that the solutions may not return to the sliding surface. Under ideal operating conditions, we can show that, in the boost PFC circuit (operating with a finite load resistance), the solutions, which fail to satisfy the local existence condition but satisfy

$$\psi_5 \frac{\mathrm{d}}{\mathrm{d}t} \left(\overline{\lambda_1}(t)\psi_3 - \overline{\lambda_2}x_1 \right) \leq 0 \quad \left(\overline{\lambda_1}(t) = \frac{\lambda_1(t)}{\omega_{ii}\,\omega_{pi}}, \; \overline{\lambda_2} = \frac{\lambda_2}{\omega_{ii}\,\omega_{pi}} \right) \tag{38}$$

cannot remain in the saturated region. Qualitatively, inequality (38) shows that, for the boost PFC circuit, if the dynamic response (or bandwidth in a linearized sense) of the voltage loop is much slower than that of the current loop, then the steady-state solution in the saturated region is virtual. If inequality (38) is satisfied, then we can show that, even though the local existence condition is not always satisfied, a spiraling motion, as shown in Figure 4(b), may be achieved.

5. EXTENSION OF THE ANALYSIS TO THE REGULARIZED PROBLEM

We rewrite the dynamic equations of the closed-loop boost PFC circuit described by equations (1)–(4) as a vector equation in the form

$$\dot{\xi} = l_1(\xi, t) + l_2(\xi, t)u \qquad \left(g_1(x_1, u) \neq 0 \right) \tag{39}$$

where $\xi = \begin{bmatrix} x_i & \psi_j \end{bmatrix}^{\mathrm{T}}$ and $\dim(\xi) = 4 \times 1$ (or 5×1). For the closed-loop system operating with controller I, using equations (1), (3), and (20), we obtain u (in a general form)

$$u = [q_2(\xi, t)]^{-1} \left(\dot{\sigma}_1 - q_1(\xi, t) \right) \tag{40}$$

by replacing ψ and x with ξ. Substituting equation (40) into equation (39), we obtain

$$\dot{\xi} = l_1(\xi, t) + l_2(\xi, t) \left([q_2(\xi)]^{-1} \left(\dot{\sigma}_1 - q_1(\xi, t) \right) \right). \tag{41}$$

The integral equation equivalent to equation (41) is

$$\xi(t) = \xi(t_0) + \int_{t_0}^{t} \left[l_1(\xi, \tau) - l_2(\xi)[q_2(\xi, \tau)]^{-1} q_1(\xi, \tau) \right] \mathrm{d}\tau$$

$$+ \int_{t_0}^t l_2(\xi)[q_2(\xi,\tau)]^{-1}\dot{\sigma}_1 \mathrm{d}\tau. \qquad (42)$$

If $\dot{\sigma}_1 = 0$ then equation (42) reduces to

$$\xi^*(t) = \xi^*(t_0) + \int_{t_0}^t \left[l_1(\xi^*,\tau) - l_2(\xi^*)[q_2(\xi^*,\tau)]^{-1}q_1(\xi^*,\tau) \right] \mathrm{d}\tau \qquad (43)$$

which describes the dynamics of the system on the sliding surface. We subtract equation (43) from equation (42), use the triangle inequality property of the norm, and obtain the following relation for the norm of the difference:

$$\begin{aligned}
\|\xi - \xi^*\| &\leq \|\xi(t_0) - \xi^*(t_0)\| + \left\| \int_{t_0}^t \left[l_1(\xi,\tau) - l_2(\xi)[q_2(\xi,\tau)]^{-1}q_1(\xi,\tau) \right] \mathrm{d}\tau \right. \\
&\quad \left. - \int_{t_0}^t \left[l_1(\xi^*,\tau) - l_2(\xi^*)[q_2(\xi^*,\tau)]^{-1}q_1(\xi^*,\tau) \right] \mathrm{d}\tau \right\| \\
&\quad + \left\| \int_{t_0}^t l_2(\xi)[q_2(\xi,\tau)]^{-1}\dot{\sigma}_1 \mathrm{d}\tau \right\|.
\end{aligned} \qquad (44)$$

If we choose $\|\xi(t_0) - \xi^*(t_0)\| = R_1\triangle$ (where $\triangle$ is the width of the boundary layer, which is assumed to be fixed just for the following expression), then we reduce equation (44) using a theorem on page 16 of Utkin (1992) to

$$\|\xi - \xi^*\| \leq R_1\triangle + \int_{t_0}^t L\|\xi(\tau) - \xi^*(\tau)\|\mathrm{d}\tau \qquad (R_1 > 0) \qquad (45)$$

provided that a Lipschitz constant L exists for $l_1(\xi^*,t) - l_2(\xi^*)[q_2(\xi^*,\tau)]^{-1}q_1(\xi^*,t)$ and $\|l_1(\xi,t) + l_2(\xi)u\| \leq W_1 + W_2\|\xi\|$ $(W_1 > 0, W_2 > 0)$. Using the Bellman–Gronwall lemma (Khalil, 1996), we can further reduce equation (45) to

$$\|\xi - \xi^*\| \leq R_2\triangle \qquad (R_2 > 0). \qquad (46)$$

It follows from inequality (46) that as $\triangle \to 0$ then $\xi \to \xi^*$. Hence, if the initial conditions of the differential equations describing the real and ideal sliding motions are sufficiently close, then their solutions are also close. We can extend the same procedure for the closed-loop system operating with controller II.

Inequality (46), however, does not give any idea about the dynamics of the nonlinear system if the two initial conditions are not sufficiently close. In other words, inequality (46) does not give any information regarding the mechanism of instability if there is one. We, therefore, extend the analysis in Section 4 to the operation of the boost PFC circuit with a finite frequency f_s. The solution of this regularized problem is defined everywhere (in a limiting sense) except at the point defined by $\psi_5 = v_r(t)$. At this point, the derivative of the solution is not defined. Such discontinuities do not occur more than once in each switching cycle. However, the states match at this point. Therefore, using the concept of the Lebesgue measure, we can obtain a numerical solution (almost everywhere) to this system.

Let us consider the closed-loop boost PFC circuit operating with controller II. For a given switching structure (i.e., for a given $g_1(x_1, u), u$), the closed-loop equations (1)–(5) can be rewritten as

$$\dot{\xi} = A(t)\xi + B_1|v_{in}(t)| + B_2 V_{dcref} \tag{47}$$

where A is a square matrix, B_1 and B_2 are column matrices, $\xi = \begin{bmatrix} x_i & \psi_j \end{bmatrix}^{\mathrm{T}}$, and dim($\xi$)=5 × 1. The solution of equation (47) is

$$\xi = \begin{cases} e^{\int_{t_0}^{t} A(\tau)d\tau} \xi(t_0) + \int_{t_0}^{t} e^{\int_{\tau}^{t_0} A(\gamma)d\gamma} B_1 v_{in}(\tau)d\tau \\ \qquad + \int_{t_0}^{t} e^{\int_{\tau}^{t_0} A(\gamma)d\gamma} B_2 V_{dcref}\, d\tau \quad \text{if } v_{in}(\tau) > 0 \\ e^{\int_{t_0}^{t} A(\tau)d\tau} \xi(t_0) - \int_{t_0}^{t} e^{\int_{\tau}^{t_0} A(\gamma)d\gamma} B_1 v_{in}(\tau)d\tau \\ \qquad + \int_{t_0}^{t} e^{\int_{\tau}^{t_0} A(\gamma)d\gamma} B_2 V_{dcref}\, d\tau \quad \text{if } v_{in}(\tau) < 0 \end{cases} \tag{48}$$

Obviously, the integrals in equation (48) cannot be computed in closed form. We can use the method of successive approximations to obtain an approximate state-transition matrix using

$$e^{\int_{t_0}^{t} A(\tau)d\tau} = I_5 + \int_{t_0}^{t} A(\tau_0)d\tau_0 + \int_{t_0}^{t} A(\tau_0) \int_{t_0}^{\tau_0} A(\tau_1)d\tau_1 d\tau_0$$

$$+ \int_{t_0}^{t} A(\tau_0) \int_{t_0}^{\tau_0} A(\tau_1) \int_{t_0}^{\tau_1} A(\tau_2)d\tau_2 d\tau_1 d\tau_0 + \cdots \tag{49}$$

where I_5 is the identity matrix of dimension 5 × 5. If we make one further assumption that $v_{in}(t)$ does not vary appreciably in a small interval, then, using equations (48) and (49), we obtain a closed-form expression for $\xi(t)$. Alternately, if we assume that both $A(t)$ and $v_{in}(t)$ do not vary appreciably in this small interval, then equation (48) reduces to

$$\xi = \begin{cases} e^{At} \xi(t_0) + \left(e^{At} - I\right)A^{-1}B_1 v_{in}(t_0) \\ \qquad + \left(e^{At} - I\right)A^{-1}B_2 V_{dcref} \quad \text{if } v_{in}(t_0) > 0 \\ e^{At} \xi(t_0) - \left(e^{At} - I\right)A^{-1}B_1 v_{in}(t_0) \\ \qquad + \left(e^{At} - I\right)A^{-1}B_2 V_{dcref} \quad \text{if } v_{in}(t_0) < 0 \end{cases} \tag{50}$$

Thus, using either equation (48) or (50) and (2) and (5), we find an approximate solution to the dynamical equations of the closed-loop boost PFC circuit in a small interval of time.

On the other hand, if we assume that $v_{in}(t)$ is a harmonic function (e.g., $V_m \cos(\omega t)$, where ω and V_m are the frequency and amplitude of the line voltage), then we obtain a closed-form solution of equation (47) spanned over one switching cycle. Since $v_{in}(t)$ is periodic,

$$\frac{1}{t} \int_0^t |v_{in}(\tau)|^2 d\tau = \frac{V_m^2}{\pi} \int_0^\pi |\cos(\omega\tau)|^2 d\tau = \text{constant.} \tag{51}$$

Hence the coefficients $\lambda_1(t)$ and $\lambda_4(t)$ are constants. Let us define two additional fictitious states ξ_6 and ξ_7 as

$$
\begin{aligned}
\xi_6 &= V_m \cos(\omega t), \\
\xi_7 &= \dot{\xi}_6 = -\omega V_m \sin(\omega t) \\
&\Rightarrow \dot{\xi}_7 = -\omega^2 \xi_6.
\end{aligned}
\tag{52}
$$

Then equation (52) changes equation (47) to the form

$$
\dot{\xi}' = A'(\xi_6)\xi' + B_2' V_{dcref}
\tag{53}
$$

where $\xi' = [\xi \quad \xi_6 \quad \xi_7]^{\mathrm{T}}$. If $v_{in}(t)$ is periodic having harmonics besides the fundamental frequency ω, then the procedure in equation (50) can be extended with additional fictitious states representing the additional harmonic terms in $v_{in}(t)$.

In equation (53), the equations governing $\dot{\xi}_1, \dot{\xi}_2, \dot{\xi}_3, \dot{\xi}_6,$ and $\dot{\xi}_7$, represented by $\dot{\xi}''$, do not possess cross couplings of the states. Because the equation governing $\dot{\xi}''$ is time invariant, its solution can be expressed as

$$
\xi'' = e^{A''t} \; \xi''(t_0) + (e^{A''t} - I_5)(A'')^{-1} B_2'' V_{dcref} \; .
\tag{54}
$$

Once we obtain ξ'', we use it to obtain ξ_4 and ξ_5. The solution of $\xi_4(= \psi_4)$ is

$$
\xi_4 = \xi_4(t_0) + \int_{t_0}^{t} g(\tau)\mathrm{d}\tau
\tag{55}
$$

where

$$
g(\tau) = P_1 M \underline{\xi}'' + P_6 M \underline{\xi}'' P_3 M \underline{\xi}''.
\tag{56}
$$

In equation (56), P_1 and P_6 are suitable row vectors and M is a matrix whose columns are the eigenvectors of A'', such that

$$
\underline{\xi}'' = M^{-1}\xi'' = e^{J\tau} M^{-1}\xi(t_0) + (e^{J\tau} M^{-1} - M^{-1})(A'')^{-1} B_2' V_{dcref}
\tag{57}
$$

where J is the Jordan form of A''. The advantage of using the Jordan form in equation (57) is that it simplifies the analysis. Substituting equation (57) into equation (56) and with little simplification, we can reduce the number of terms in equation (56) to six. Five of these terms, when integrated using equation (55) give a closed-form solution. The sixth is integrated term by term. We performed this integration easily using MATHEMATICA. Thus, using a little mathematical manipulation, we solved ξ_4 exactly. Once ξ_4 and ξ'' are known, we solve for $\xi_5(= \psi_5)$ exactly using a procedure similar to that used for solving ξ_4. The solution of ξ obtained using the above procedure is exact. This could be particularly helpful in the analysis when the switching frequency and the line frequency are not wide apart. It can also be used to find the accuracy of numerical solutions of equation (47). Using equation (57) and the expressions for ξ_4 and ξ_5, we obtain a discrete form of the solution of ξ for a given switching topology as

$$\xi_{n+1} = \Phi_n \xi_n + \Gamma_n V_{dcref} \ . \tag{58}$$

The closed-loop converter has two fundamental frequencies: the forcing frequency and the switching frequency. Hence, the dynamics of the discontinuous system evolve over a torus. Using a first-order Poincaré map, we obtain a reduced-order system that has no discontinuity due to control. The first-order Poincaré map is obtained by generating a map, which relates the values of the states ξ at the end of a switching cycle to those at the beginning of the next cycle (Alfayyoumi et al., 1999; Mazumder et al., 2001). To obtain this map, we stacked the solution in equation (58) for two consecutive switching topologies (if the converter is in CCM) or for three consecutive switching topologies (if the converter is in DCM). The switching instant in any switching cycle is obtained by solving a transcendental equation of the form

$$\rho(\xi_n, t) - V_m = 0. \tag{59}$$

The validity of the results obtained with the first-order Poincaré map is up to half the switching frequency. The stability of the closed-loop boost PFC circuit is verified by determining the orbital stability of the first-order map. Alternatively, we can determine the stability using a second-order Poincaré map, which is generated by taking a transversal section of the first-order map. The advantage of the second-order map is that the problem of determining the stability of an orbit is reduced to determining the stability of a point. However, the stability analysis is valid only for the reduced-order problem.

6. RESULTS

The power stage and multi-loop controller parameters used to obtain the experimental and simulation results are listed in Tables 1 and 2. Due to lack of space and to avoid repetition, all the results in this section (except for Figure 10) are obtained using the second current-loop controller, which is being commercially used. We begin with Figure 5, which shows that, even when the width of the boundary layer approaches zero, the existence condition fails at $x_1 = 0$. This is evident from the jumps in the values of ψ_5 and $(\psi_5 \dot{\psi}_5)$ at that point. Hence, global existence of a smooth hypersurface in a boost PFC circuit is not possible.

When the existence condition fails, then the solutions leave the sliding surface. If these solutions do not satisfy (38), then they remain in the saturated region permanently. To demonstrate this, we designed a closed-loop system with a fast voltage loop so that condition (38) is violated. Figure 6 shows that ψ_5 continues to increase and hence, u remains permanently at a value of one. As a result the capacitor voltage continues to decay until it stabilizes at a value zero, which is the equilibrium state for the capacitor voltage in this saturated region. We should note that, in a real boost PFC circuit, the fault-handling systems will shut down the converter prior to this outcome.

The boost PFC circuit is used as a universal power supply. In other words, it should be stable even if the root-mean-square (rms) value of the input voltage varies between 90 V (low line) to 265 V (high line). In Figure 7, we show that, for a finite frequency of operation (90 kHz), a fast-scale instability (in the vicinity of $x_1 = 0$) occurs earlier for low line. Under normal operating conditions, the third term in equation (34) is quite small. Hence, as $|v_{in}(t)| \to 0$, $u_{eq} \to 1$. Thus, it follows from equation (21) that for a low line, $u_n \to 0$
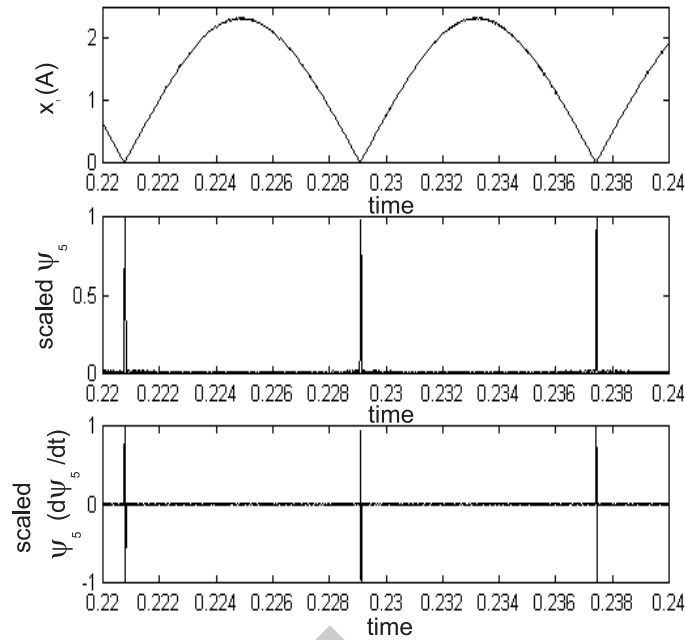
Figure 5. The existence condition fails at $x_1 = 0$, thus only local existence is possible for the boost PFC circuit.
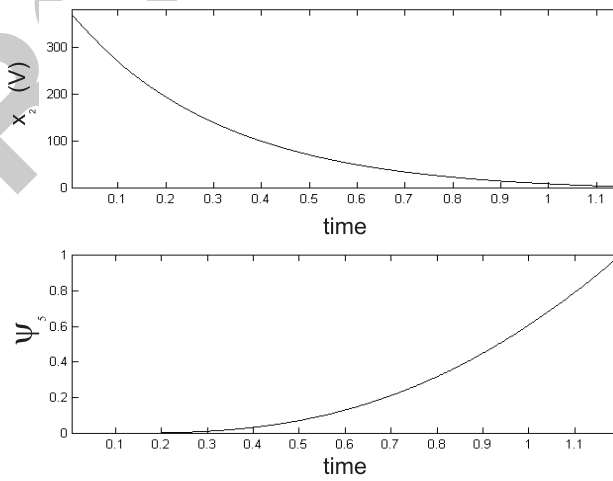

Figure 6. Condition (38) is violated and hence the solution leaves the local sliding surface.
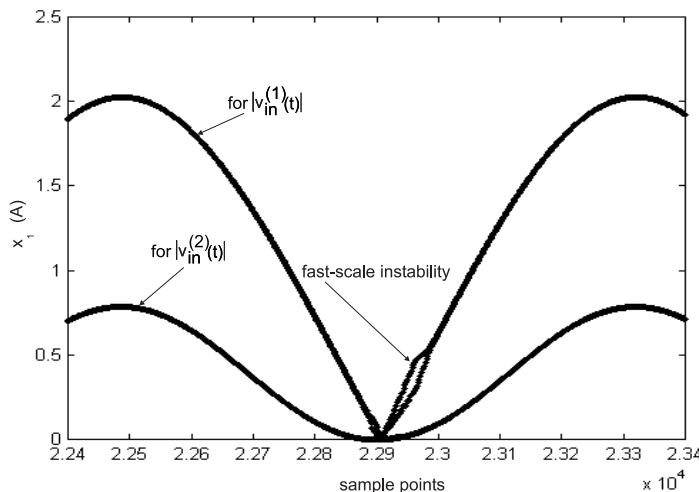
Figure 7. Using a first-order Poincaré map we show that a fast-scale instability occurs for a lower input voltage ($|v_{in}^{(1)}(t)|_{max} < |v_{in}^{(2)}(t)|_{max}$) when all other parameters are kept the same.

faster as the input voltage decreases and hence the (local) existence condition for a sliding manifold may be violated earlier, which results in an earlier onset of instability. On the other hand, using equations (25) and (34), we can also show that when $|v_{in}(t)|_{max} \rightarrow x_2$, $u_{eq} \rightarrow 0$ and condition (25) will be violated. Hence the system is vulnerable to instability because the local existence condition may fail. This instability will occur earlier for high line. In Figure 8, we show that a boost PFC circuit (whose controller gains have not been optimized) loses stability on a fast scale as the input voltage is increased from low line to high line. In Figure 9, we show that, when $|v_{in}(t)|_{max} \rightarrow x_2$ and the current-loop controller gain ($\propto k$) is high, a fast-scale instability occurs not only at the peak of the current but also when it approaches zero. This result can be explained, as before, using equations (25) and (34).

In Figure 10 we show that, if the switching of the boost PFC circuit is based on $\psi_6 = 0$ rather than on $\psi_5 = 0$, then the stability of the system improves provided that the signal-to-noise ratio of x_1 is high. For these two cases, the results agree with the explanation given in Section 4 using the local existence conditions (28) and (36).

Finally, using a first-order Poincaré map, we explore the mechanism of the fast-scale instability when the converter is operated with a finite frequency of 90 kHz and the current-loop controller gain ω_{ii} (see Figure 1) is gradually increased. We show in Figure 11 that, as ω_{ii} is increased, a fast-scale instability occurs in the vicinity of the point $x_1 = 0$. The fast-scale instability doubles the switching period, which ultimately leads to chaos. In Figure 12, we show experimental results confirming the existence of the fast-scale instability. The figure shows doubling of the switching period. We note that, when the switching frequency of the converter is finite, then the dynamics of the closed-loop system evolve on a torus. Hence the instabilities, in Figure 11, actually show projections of the torus breakdown.

We note that unlike dc–dc converters, the boost PFC circuit exhibits period-two, period-four, higher-order periods, and chaotic dynamics in one line cycle due to the time variation in $|v_{in}(t)|$. Interestingly, when we analyzed the closed-loop system using Floquet theory
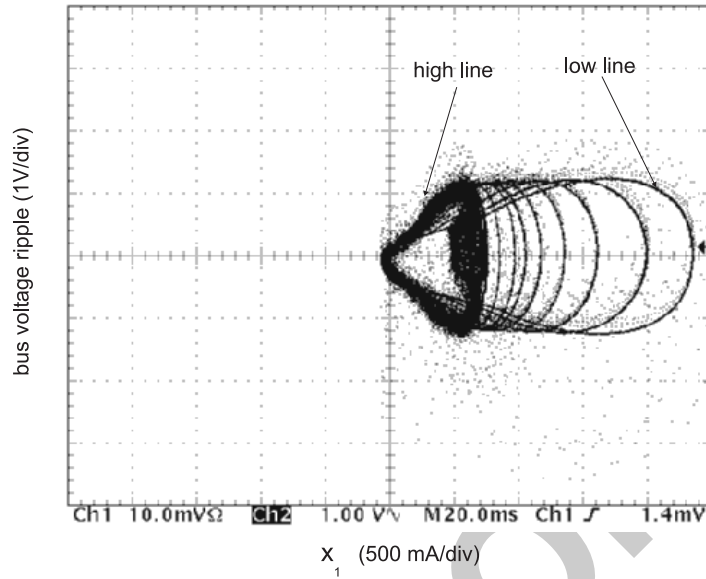
Figure 8. An experimental result, which shows that, if the controller gains are not properly optimized, then the onset of a fast-scale instability occurs when $|v_{in}(t)|_{max} \to x_2$.
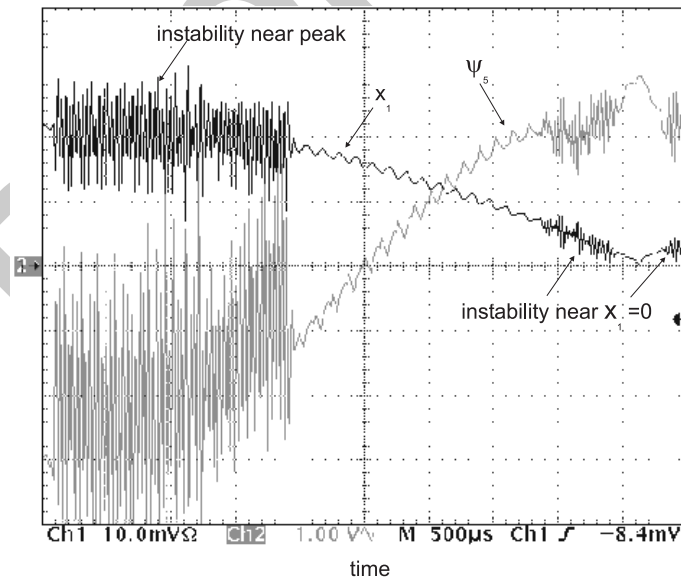

Figure 9. An experimental result, which shows that, if the controller gains are not properly optimized, then the boost PFC circuit becomes unstable on a fast scale not only when $x_1 \to 0$ but also when $|v_{in}(t)|_{max} \to x_2$.
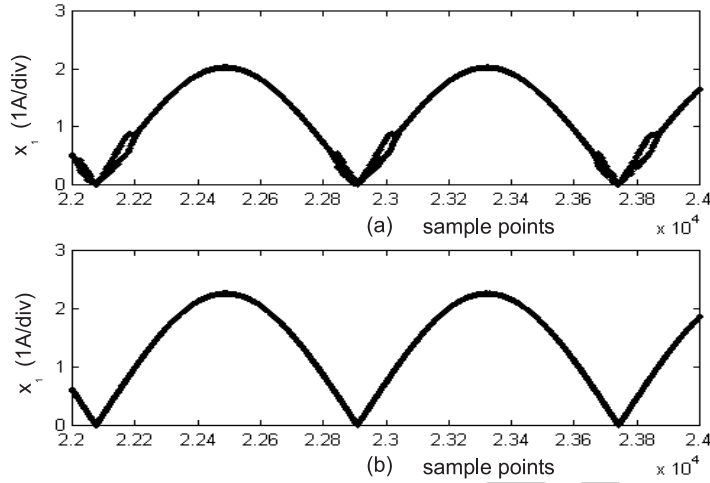
Figure 10. Performance of the boost PFC circuit on the fast scale: (a) switching based on $\psi_5 = 0$ and (b) switching based on $\psi_6 = 0$.
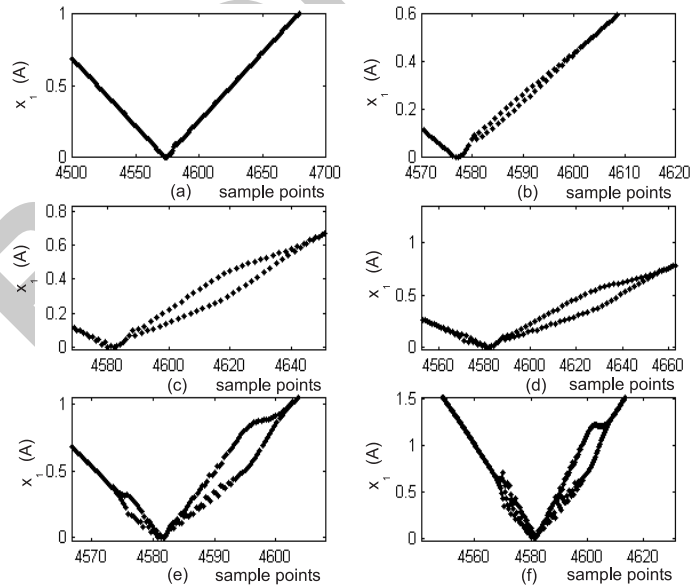

Figure 11.   Results based on a first-order Poincaré map, which show the onset and progress of a fast-scale instability as ω_{ii} is increased. The fast-scale instability occurs via a period doubling of the switching period, which ultimately leads to chaos.
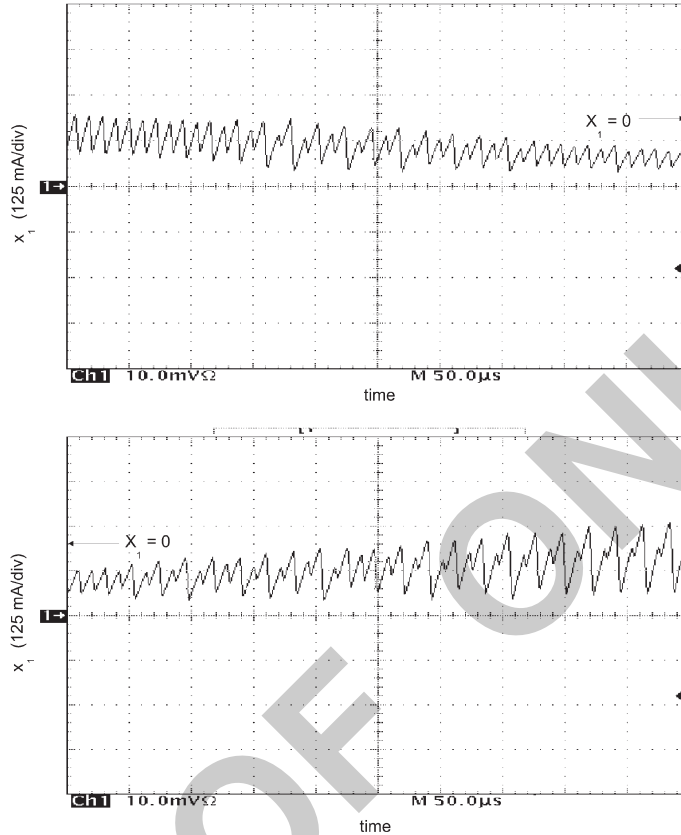
Figure 12. An experimental result which confirm the fast-scale instability near $x_1 = 0$. The fast-scale instability results in a period doubling of the ripple of the inductor current x_1 in these cases.

(based on a second-order Poincaré map), we found all the four cases in Figure 11 to be stable. Clearly this is not the case. The reason behind this fallacy is that, using a second-order Poincaré map, we can predict orbital instability only on the slow scale (Kaas-Peterson, 1986; Wang, 1997).

7. SUMMARY AND CONCLUSION

We investigate the stability of a discontinuous, time-varying boost PFC circuit operating with a multi-loop controller. We treat two separate cases: one for which the switching frequency is infinite and the other for which the switching frequency is finite but large. We show that, even when the frequency is approaching infinity, the existence condition is violated when $x_1 = 0$.

Having shown that global existence is not possible, we develop conditions for local existence using Lyapunov functions. We show that, for the closed-loop system operating with controller I, the local existence condition (28) is satisfied as long as the nonlinear control

u_n satisfies equation (29). However, for the boost PFC circuit operating with controller II, the existence condition (36) is difficult to satisfy. The reason behind this difficulty is that, while the desired sliding motion ($\ddot{\psi}_5 = 0$) is second order in nature, the control is based on ψ_5, which along with $\dot{\psi}_5$ are both continuous functions. Although the control effort for this case is lower than that in the previous case, the closed-loop system is more susceptible to fast-scale instabilities when the frequency is not infinite.

For the closed-loop system operating with controller II, using the local existence conditions and the concept of equivalent control, we show why fast-scale instabilities near the point $x_1 = 0$ may occur earlier for a lower line voltage. We also show that, if the controllers are not properly optimized, then the boost PFC circuit loses stability on a fast scale when $x_1 \to 0$ and also when $|v_{in}(t)|_{max} \to x_2$. When a trajectory leaves a sliding surface, it may or may not remain in the saturated region permanently. We show in equation (38) a condition that ensures the nonexistence of a real equilibrium trajectory in the saturated region under ideal conditions. The design implication of this is that, for the given closed-loop system, the dynamic response (or the bandwidth in a linearized sense) of the voltage loop must be slower than that of the current loop.

For a converter operating with a finite switching frequency, there is a boundary layer around the region of discontinuity. Therefore, we do not have to deal with generalized solutions. Using controller II (as an example), we show two different approaches for obtaining a solution for the closed-loop system. We find that, within the boundary layer, the dynamics of the nonlinear system evolve on a torus. The toroidal dynamics have two fundamental frequencies: the frequency of $v_{in}(t)$ and the switching frequency. Using a first-order Poincaré map, we show how the closed-loop system loses stability on a fast scale in the neighborhood of $x_1 = 0$ as the controller gain for the current loop increases. Using the slope of x_1, we show that the fast-scale instability results in a doubling of the switching period. The existing averaged models of the boost PFC circuit, most of which are designed to predict the slow-scale dynamics, do not predict these fast-scale instabilities until the subharmonics (in a linearized sense) of the switching frequency affect the slow scale as well.

We come to several conclusions. First, analysis of the stability of the boost PFC circuit must predict the behavior of the closed-loop system in the unsaturated and saturated regions. While saturated regions always exist, conditions for the existence of the unsaturated regions have to be established. We cannot simply substitute a continuous function for a pulse function, as is conventionally done. Secondly, an analysis based on the discontinuous converter (operating without a diminishing boundary layer) offers good guidelines regarding conditions for the onset of instabilities in the boost PFC circuit operating with a large but finite frequency. Still, we have to analyze the toroidal dynamics inside the boundary layer to determine the actual onset of instabilities and their mechanisms. One approach involves the use of a discrete Lyapunov function. This is difficult because most nonlinear systems do not have closed-form solutions. The other approach involves a bifurcation analysis using a projection operator (e.g., Poincaré map). Using these concepts derived from the analysis of nonlinear and discontinuous systems, we have shown in this paper the potential of significantly improving the stability analysis of not only boost PFC circuits but also of other converters of similar class. Thirdly, the choice of a sliding surface should be carefully done. We should keep in mind the compromise between control effort and stability. Finally, the stability analyses in this paper show the inability of existing linear controllers to provide global stability.

REFERENCES

Alfayyoumi, M., Nayfeh, A.H., and Borojević, D., 1999, "Input filter interactions in dc–dc switching regulators," in *IEEE Power Electronics Specialists Conference* pp. 926–932.

Andreycak, B., 1997, "Advanced power factor correction control ICs," *Unitrode Inc.*, Design Note DN-44.

Chang, L.W., 1990, "A MIMO sliding control with a second order sliding condition." in *ASME WAM*, Paper No 90-WA/DSC-5, Dallas, TX.

Elmali, H. and Olgac, N., 1992, "Robust output tracking control of nonlinear MIMO systems via sliding mode technique." *Automatica* **28**, 145–151.

Erickson, R.W., Ćuk, S., and Middlebrook, R.D., 1982, "Large-signal modelling and analysis of switching regulators," in *IEEE Power Electronics Specialists Conference* pp. 240–250.

Filippov, A.F., 1988, *Differential Equations with Discontinuous Righthand Sides*, Kluwer, Dordrecht.

Hahn, W., 1963, *Theory and Application of Liapunovs Direct Method*, Prentice-Hall, Englewood Cliffs, NJ.

Henze, C.P. and Mohan, N., 1986, "A digitally controlled AC to DC power conditioner that draws sinusoidal input current," in *IEEE Power Electronics Specialists Conference* pp 531–540.

Huliehel, F.A., Lee, F.C., and Cho, B.H., 1992, "Small-signal modeling of the single-phase boost high factor converter with constant frequency control," in *IEEE Power Electronics Specialists Conference* pp. 475–482.

Kaas-Petersen, C., 1986, "Computation of quasi-periodic solutions of forced dissipative systems," *Journal of Computational Physics* **58**, 395–408.

Khalil, H.K., 1995, *Nonlinear Systems*, 2nd edition, Prentice-Hall, Englewood Cliffs, NJ.

Mazumder, S., Nayfeh, A.H., and Borojević, D., 2001, "A theoretical and experimental investigation of the fast- and slow-scale instabilities of a dc–dc converter." in *IEEE Transactions on Power Electronics* **16**, 201–216.

Mazumder, S., Nayfeh, A.H., and Borojević, D., 2002, "Robust control of parallel dc–dc buck converters by combining integral-variable-structure and multiple-sliding-surface control schemes," *IEEE Transactions on Power Electronics* in press.

Mohan, N., Undeland, T.M., and Ferraro, R.J., 1984, "Sinusoidal line current rectification ith a 100kHz B-SIT step-up converter," in *IEEE Power Electronics Specialists Conference* pp. 92–98.

Nayfeh, A.H. and Balachandran, B., 1995, *Applied Nonlinear Dynamics*, Wiley, New York.

Ridley, R.B., 1989, "Average small-signal analysis of the boost power factor correction circuit," in *Proceedings of the Virginia Power Electronics Seminar* pp. 108–120.

Simonetti, D., Sebastiań J., Cobos, J.A., and Uceda, J., 1995, "The continuous-discontinuous conduction boundary of a boost PFP fed by universal input," in *CIEP* pp. 20–24.

Todd, P, 1999, "UC3854 controlled power factor correction circuit design," *Unitrode Inc.*, Application Note U-134.

Utkin, V.I., 1992, *Sliding Modes in Control Optimization*, Springer-Verlag, New York.

Wang, X., 1997, "Analytical methods of nonsynchronous response and bifurcation in nonlinear rotordynamics with applications," Ph.D. Dissertation, Department of Mechanical Engineering, Texas A&M University, College Station, TX.

Williams J.B., 1989, "Design of feedback loop in unity power factor ac to dc converter," in *IEEE Power Electronics Specialists Conference* pp. 959–967.

Zhou, C. and Jovanović, M.M., 1992, "Design trade-offs in continuous current-mode controlled boost power factor correction circuits," in *Proceedings of the High-Frequency Power Conversion Conference* pp. 209–220.

Zhou, C., Ridley, R.B., and Lee, F.C., 1990, "Design and analysis of a hysteretic boost power factor correction circuit," in *IEEE Power Electronics Specialists Conference* pp. 800–807.